CHEMISTRY OF MATERIALS

pubs.acs.org/cm

Article

N-Heterocyclic Carbene-Stabilized Gold Nanoparticles: Mono- Versus Multidentate Ligands

Neda Arabzadeh Nosratabad, Zhicheng Jin, Liang Du, Mannat Thakur, and Hedi Mattoussi*

Cite This: *Chem. Mater.* 2021, 33, 921−933

Read Online

ACCESS | Metrics & More | Article Recommendations | Supporting Information

ABSTRACT: Over the past decade, N-heterocyclic carbenes (NHCs) have attracted remarkable attention as metal-coordinating ligands because of their ability to strongly interact with transition metal complexes and surfaces. We investigate the coordination interaction between colloidal gold nanoparticles (AuNPs) and three sets of hydrophilic NHC-based ligands: an amine-modified small molecule, a monomeric NHC appended with a poly(ethylene glycol) (PEG) block, and a modified poly(isobutylene-*alt*-maleic anhydride), PIMA, that simultaneously presents multiple NHC groups and several short PEG chains. In this report, we find that all three ligands can rapidly coordinate onto AuNPs, as characterized using a combination of NMR spectroscopy, high-resolution transmission electron microscopy, and dynamic light scattering. These measurements have been supplemented with colloidal stability tests as well as competition from dithiothreitol molecules. Overall, we find that multidentate NHC polymer coating exhibits the highest affinity to AuNPs, which manifests in long-term colloidal stability in buffer media, absence of any aggregation, and better resistance to competition from reducing molecules. We further exploit these data to infer additional insights into the interaction and coordination of NHC molecules with Au surfaces.

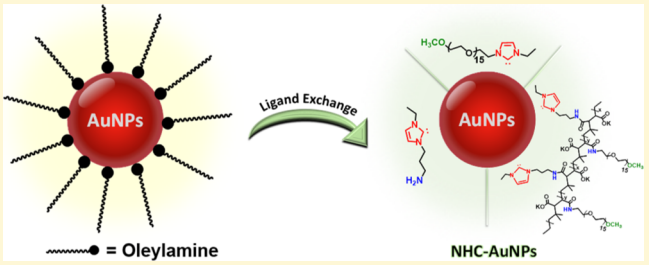

INTRODUCTION

Among the variety of solution-phase grown inorganic nanocrystals, gold nanocolloids are one of the most stable materials and they exhibit fascinating properties, including unique size- and shape-dependent photophysical properties and strong fluorescence quenching of proximal fluorophores.[1−6] Gold colloids have also been shown to promote plasmon-enhanced fluorescence combined with decrease in the lifetimes of dyes under certain proximity conditions.[7,8] These properties combined with the great chemical stability have made gold colloids a model system of choice for use in various applications. These include surface-enhanced Raman scattering, biological sensing, imaging, theranostics, and photodynamic therapy to treat cancers.[2,9−14] Growth of these materials using either hydrophilic or hydrophobic conditions yields nanocolloids that are not readily compatible with biological systems because of either the hydrophobic nature of the ligands or the labile properties of the coatings.[15,16] Regardless of the growth route used, modification of the surface coating is required to render these nanostructured materials hydrophilic and colloidally stable in a wide range of conditions.[17,18] Cap exchange, which relies on substituting the original coating with bifunctional hydrophilic ligands, is one of the most effective strategies for promoting the dispersion of various inorganic nanocrystals in biological media. Overall, effectiveness of the coating strategy is determined by the strength of the coordination interactions and affinity of the hydrophilic moieties to the surrounding media.[19]

For decades, thiol-modified ligands have been widely employed for the stabilization of gold nanocolloids because their coordination onto Au surfaces is strong.[20] More recently, N-heterocyclic carbenes (NHCs) have attracted increasing attention as alternative ligands for coating Au and other nanocolloids.[21−24] Using the hard and soft acids and bases principle is informative for rationalizing the coordination affinity of NHC groups to Au nanocolloids.[25] Given its ability to share two electrons, NHC is considered a soft Lewis base, which implies that moieties presenting this group exhibit strong affinity to gold and other transition metal nanocrystal surfaces because of the soft Lewis acidic character of these materials.[24,26−28] Indeed, covalent interactions have been proposed to characterize NHC-to-gold nanoparticle (AuNP) binding. NHC molecules have been explored as stabilizing agents for transition metal-rich NPs (e.g., those with cores made of Au,[29−32] Ru,[33,34] Pd,[35,36] Co,[37] and Ir[38]) and upconverting NPs.[39] In addition, using well-thought synthetic rationales, NHCs can be easily modified by attaching diverse functional groups to finely tune their steric and electronic properties.[25,40] These findings have

Received: October 5, 2020
Revised: January 8, 2021
Published: January 23, 2021

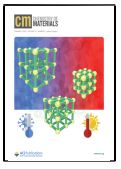

https://dx.doi.org/10.1021/acs.chemmater.0c03918
Chem. Mater. 2021, 33, 921−933

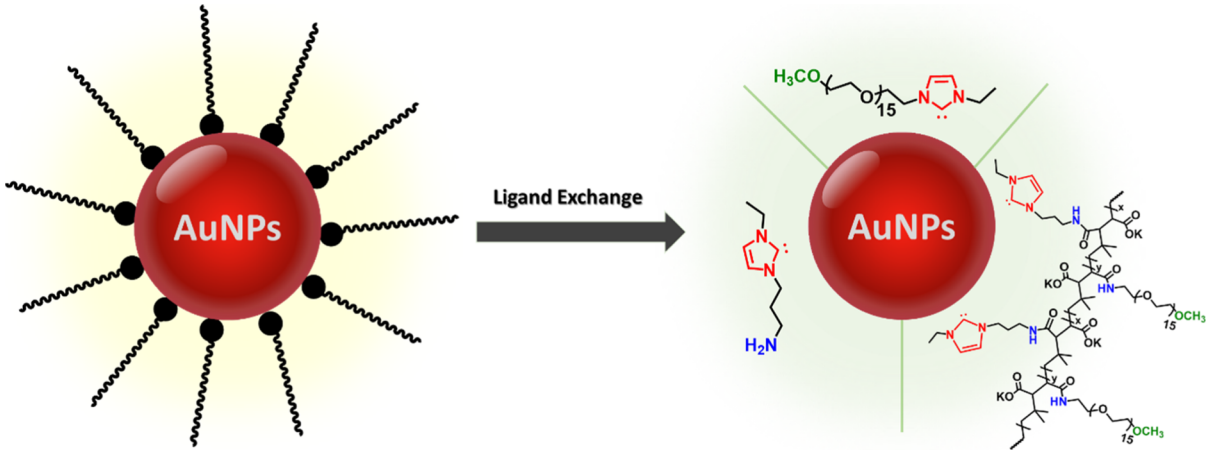

Figure 1. Schematic representation showing the ligand exchange of hydrophobic OLA-AuNPs with various NHC-based ligands and their transfer to hydrophilic media. Three sets of NHC-modified hydrophilic ligands are shown: NHC-APE, NHC-PEG, and NHC-PIMA-PEG.

made them very appealing for many research areas, including organometallic chemistry and catalysis.[34,36,41−45] Previous studies have shown that NHC-functionalized AuNPs with either bidentate NHC or NHC attached to a hydrophilic poly(ethylene glycol), PEG, moiety can provide stability to the nanocrystals over a broad range of pH buffers for a few weeks.[46−49]

Over the past few years, our group has demonstrated the importance of higher coordination ligands, such as polymer-based compounds, in promoting high binding affinity onto various core nanocolloids. Several multicoordinating ligands have been designed and tested for the coating of colloidal iron oxide nanocrystals, luminescent semiconductor quantum dots (QDs), and various Au nanostructures, where they imparted long-term steric stability onto these materials in hydrophilic as well as hydrophobic media.[50−55] Building on these observations, we reasoned that polymers that present a combination of multiple NHCs and PEG blocks would yield multicoordinating ligands that could enhance the colloidal stability of AuNPs in buffer media.

In this study, we designed, synthesized, and tested a new set of NHC-modified molecules as novel capping ligands for the stabilization of AuNPs (schematically depicted in Figure 1). In particular, three structurally distinct NHC-based ligands were prepared as follows: two monodentate ligands [one amine-alkyl-linked NHC, NHC-aminopropylethyl (APE), and one PEG-appended NHC, NHC-PEG] and a multi-NHC polymer (NHC-PIMA-PEG). Successful phase transfer of the AuNPs with these three ligands was achieved, indicating that NHC binds to the Au surface, regardless of the exact chemical structure of the ligand. However, the long-term colloidal stability of the resulting AuNPs in buffer media depends on the coordination number (i.e., number of NHC groups associated with each ligand) and the choice of the hydrophilic motif used. Accordingly, the NHC-PIMA-PEG-coated AuNPs exhibited the highest colloidal stability. Characterization of the photophysical, structural, and colloidal stabilities of the new materials was carried out using UV−vis absorption spectroscopy, ^{1}H NMR spectroscopy, transmission electron microscopy (TEM), and dynamic light scattering (DLS). Additionally, we performed colloidal stability tests using a competing reducing molecule (dithiothreitol, DTT) and compared side by side the data collected from the present set of NHC ligands with those acquired using a multi-lipoic acid ligand, LA-PIMA-PEG, prepared using the same chemical route starting with the poly(isobutylene-*alt*-maleic anhydride) (PIMA) precursor. These measurements provided insights into the effectiveness of the NHC-ligand substitution strategy.

RESULTS AND DISCUSSION

Ligand Design. As our goal is to design stable NHC-containing ligands, we have selected a commercially available imidazole derivative as the building block because it is amenable to functionalization of the two nitrogen atoms in the ring. The resulting nitrogen-bound substituents ultimately provide added kinetic stability to the final carbene species by sterically hindering dimerization to the corresponding olefin.[25] Using this approach, we designed three sets of NHC-based ligands using different chemical routes (summarized in Figure 2). The monodentate NHC ligands were synthesized in order to establish a comparison with the multidentate NHC-polymer ligand.

To prepare the first ligand, NHC-APE, we chose 1-(3-aminopropyl)imidazole (APIm) as a precursor because it presents a free NH_2 group, which would ultimately promote affinity of the ligand-coated AuNPs to water media. The ligand was prepared via the following procedure (Figure 2a). Di-*tert*-butyl dicarbonate (BOC)-protected APIm was reacted with bromoethane to yield the BOC-protected 1-(3-aminopropyl)-3-ethylimidazolium bromide (BOC-APEIm-ium). BOC deprotection under acidic conditions produced a compound presenting a free amine and an imidazolium salt (APEIm-ium). The APEIm-ium can be transformed to the corresponding NHC-appended ligand using any conventional strong base, such as alkali metal alkoxides.[56,57] In the present case, NHC-APE was produced by deprotonation of the APEIm-ium using potassium *tert*-butoxide (KOtBu), where the reaction was carried out under an inert atmosphere in anhydrous dimethyl sulfoxide. These steps have yielded the NHC-APE product in gram scale, which can be stored under N_2 atmosphere.

The second PEG-appended NHC ligand requires the attachment of a PEG_{750} block onto the NHC group to afford increased water compatibility. The synthetic steps to prepare the PEG-imidazolium salt (PEG-EIm-ium), which can ultimately be transformed after base treatment to NHC-modified PEG, are schematically summarized in Figure 2b. First, PEG-appended imidazole (PEG-Im) was synthesized via nucleophilic substitution reaction between imidazole and OMe-PEG-OMs. The

https://dx.doi.org/10.1021/acs.chemmater.0c03918
Chem. Mater. 2021, 33, 921−933

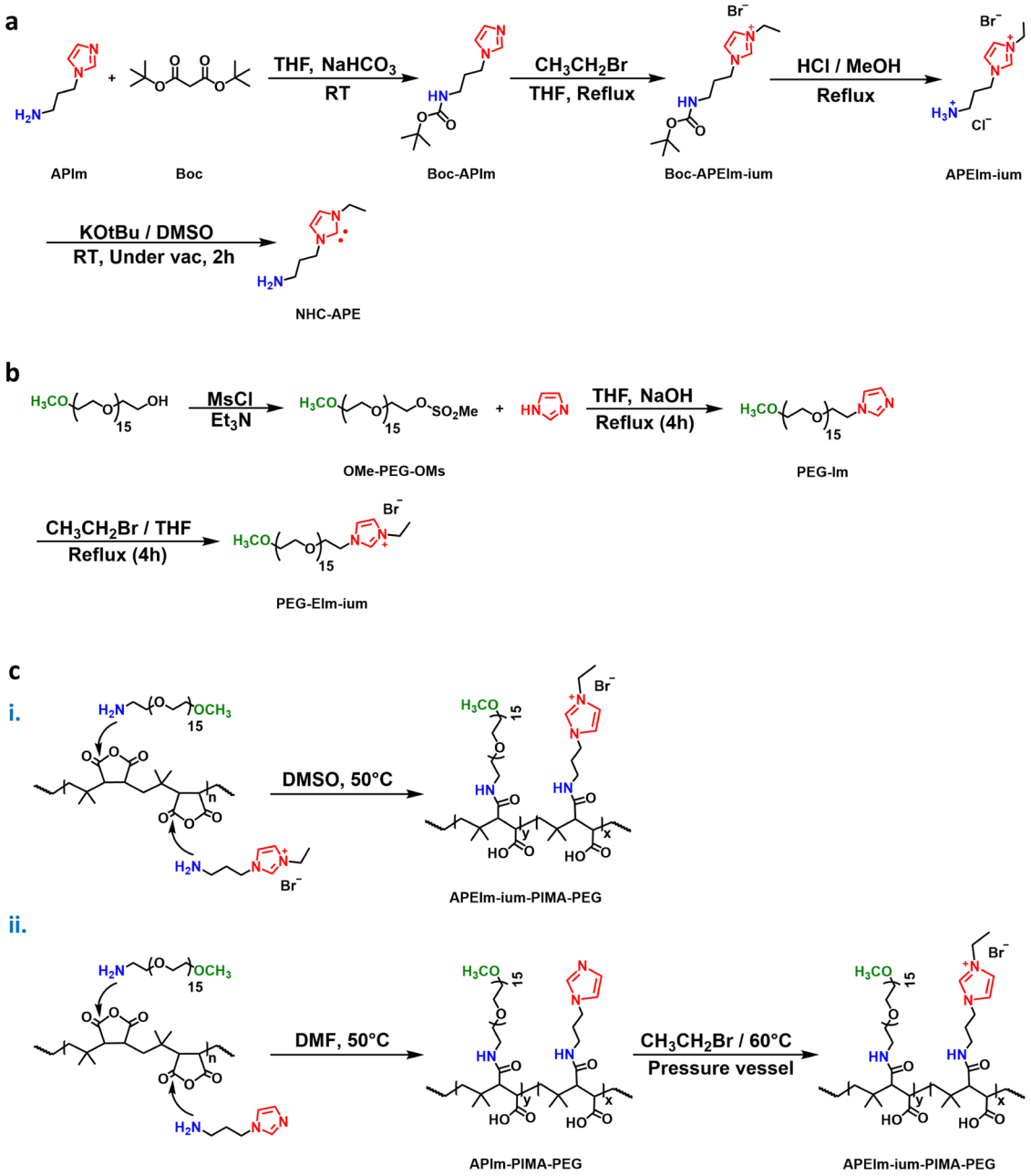

Figure 2. Synthetic routes employed for preparing the NHC-based ligands. (a) Synthesis of NHC-APE involved reaction with bromoethane, BOC deprotection, and carbene generation using KOtBu. (b) Synthesis of PEG-EIm-ium. (c) Synthesis of APEIm-ium-PIMA-PEG via two different routes: (route i) One-step nucleophilic addition reaction between PIMA and a mixture of NH_2-PEG-OMe and APEIm-ium. (route ii) This route involved two steps. In the first, APIm-PIMA-PEG was prepared via addition reaction between PIMA and a mixture of NH_2-PEG-OMe and APIm. The APIm-PIMA-PEG was then reacted with bromoethane to yield APEIm-ium-PIMA-PEG, in the second step. It should be noted that the NHC-PEG generation was carried out in the presence of the AuNPs (in situ) and thus combined with ligand exchange. Conversely, NHC-PIMA-PEG ligands were generated using either ex situ, by the deprotonation of the imidazolium salt using KOtBu, prior to mixing with the OLA-AuNPs, or in situ and combined with the ligand exchange, as done with NHC-PEG above.

latter compound was prepared by reacting OMe-PEG-OH (a PEG_{750} block was used) with methanesulfonyl chloride in the presence of triethylamine.[58,59] The resulting compound was then reacted with bromoethane to yield the PEG-EIm-ium salt. In situ conversion of this product to NHC-PEG was carried out in the presence of KOtBu during the ligand exchange process (see below).

To prepare the third set, NHC-based polymer, we first synthesized APEIm-ium-PIMA-PEG (serving as an intermediate or a precursor) using two alternative routes that rely on the one-step nucleophilic addition reaction between PIMA and amine-R nucleophiles, as summarized in Figure 2c.[54] APEIm-ium-PIMA-PEG was first prepared by reacting PIMA either with H_2N-PEG and APEIm-ium (route i) or with H_2N-PEG and APIm (route ii).[52,54,60] The molar ratio of APIm/APEIm-ium to NH_2-PEG used is 50:50, which is expected to introduce approx. ~20 APIm/APEIm-ium groups and ~20 PEG motifs per polymer ligand.

Route (i) relied on the reaction between PIMA and a mixture of presynthesized NH_2-PEG and APEIm-ium nucleophiles to

https://dx.doi.org/10.1021/acs.chemmater.0c03918
Chem. Mater. 2021, 33, 921−933

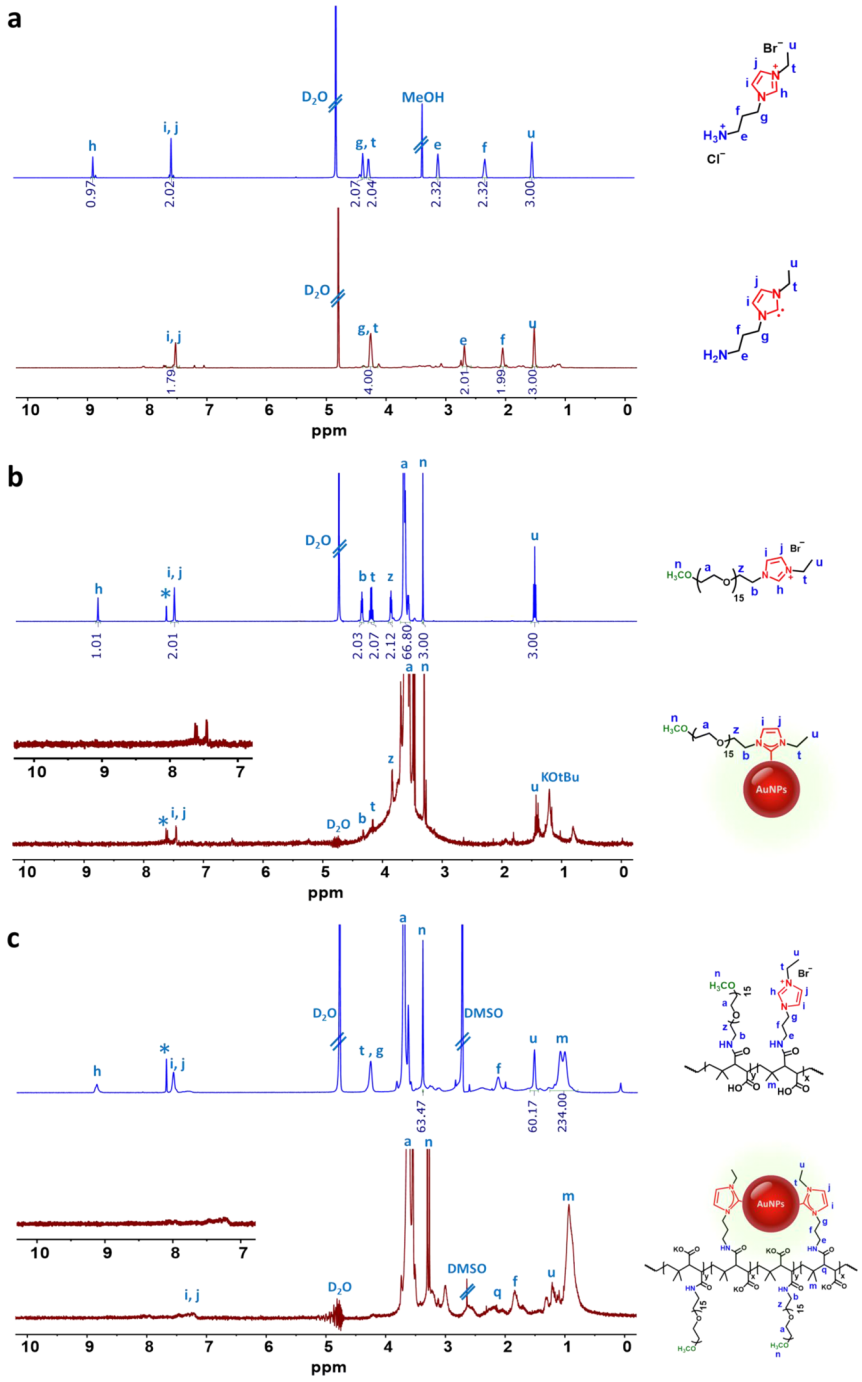

Figure 3. Stacked ^{1}H NMR spectra of (a) APEIm-ium salt precursor and NHC-APE following ex situ transformation of the imidazolium to carbene; (b) PEG-EIm-ium salt (top) and NHC-PEG-AuNPs following in situ treatment using KOtBu (bottom); (c) APEIm-ium-PIMA-PEG (top) and NHC-PIMA-PEG-AuNPs (bottom), also prepared via in situ generation using KOtBu. All samples were prepared in D_2O. Absence of the acidic hydrogen peak at 8.76 ppm is the evidence confirming generation (or installation) of the NHC ligands on the AuNP surfaces.

obtain the APEIm-ium-PIMA-PEG ligand. Conversely, route (ii) involved two reaction steps, where PIMA was first reacted with a mixture of NH_2-PEG and APIm, yielding APIm-PIMA-PEG. Then, APIm-PIMA-PEG was reacted with bromoethane to provide APEIm-ium-PIMA-PEG.

Ligand Exchange and Phase Transfer. The newly synthesized NHC-based ligands were applied for the coating of hydrophobic oleylamine (OLA)-AuNPs, which were prepared using high-temperature growth reaction.[61,62] Ligand substitution using the monodentate ligand was carried out by mixing the OLA-AuNPs dispersed in hexane with NHC-APE dissolved in chloroform; a molar excess with respect to the NP concentration of ~2,500,000-fold was used. Ligand exchange with this compound was rapid (about 5 min with shaking) and resulted in precipitation of the newly capped AuNPs, which were centrifuged into a pellet. After discarding the supernatant containing free OLA, the AuNP pellet was dispersed in water. However, despite the fact that ligand substitution was rapid and used preactivated NHC, its effectiveness was very limited. Indeed, we found that the resulting AuNPs were prone to aggregation within 10−15 min, coupled with broadening and red shifting of the surface plasmon resonance (SPR) peak (see

https://dx.doi.org/10.1021/acs.chemmater.0c03918
Chem. Mater. 2021, 33, 921−933

Supporting Information, Figure S1). We attribute this result to the inability of this ligand to impart colloidal stability to NP dispersions in water. Compatibility with water is essentially promoted by the terminal NH_2, which do not provide enough steric interactions to the colloids over a broad range of conditions (e.g., pH).[49]

Ligand exchange with NHC-PEG was carried out under in situ conditions. OLA-AuNPs and PEG-EIm-ium were first mixed in tetrahydrofuran (THF) (at 300,000-fold molar excess of the ligand with respect to AuNPs); then, the atmosphere was switched to nitrogen by applying three rounds of vacuum followed by purging with N_2. A solution of KOtBu dissolved in THF was added dropwise through a septum (over ∼15 min) to promote deprotonation of the PEG-EIm-ium salt and carbene generation in situ, which was followed by mild overnight heating at 40 °C. Subsequent processing and purification steps were carried out under atmospheric conditions. Removal of excess OLA, potassium salts, and free NHC ligands yielded NPs that were readily dispersed in deionized (DI) water. Ligand exchange under ex situ conditions, where carbene generation is first carried out on PEG-EIm-ium, prior to mixing with the OLA-AuNPs, could not be implemented.

Remark: We would like to note that introducing a small amount of polysorbate 20 (TWEEN 20) with the ligands prior to mixing with OLA-AuNP dispersions may help the ligand exchange and phase transfer steps, as suggested in ref 63 However, in our hands, we found no difference between ligand substitutions carried out with or without the addition of this surfactant.

Ligand exchange with the polymer was implemented following the steps described above for the monomer ligand either using in situ (i.e., carbene generation was carried out in the presence of AuNPs) or ex situ conditions, where carbenes were generated first in the absence of AuNPs.

For the in situ route, typically, a solution of APEIm-ium-PIMA-PEG in THF was mixed with OLA-AuNPs (precipitated in ethanol) and purged with N_2; 15,000-fold molar excess ligands with respect to AuNPs were used. Then, KOtBu dissolved in THF was added dropwise and the mixture was stirred at 40 °C overnight. It is to be noted that the molar concentration of KOtBu was ∼2 times larger than the anhydride monomer concentration in APEIm-ium-PIMA-PEG in order to account for the number of carboxyl groups (acids) freed along the PIMA chain during the ring opening reaction; this ensured that adequate amount of base was used for carbene generation. The final polymer-coated AuNPs were purified using a membrane filtration device, following the same steps used for ligation with NHC-PEG-AuNPs (see Experimental Section) to yield a homogenous NP dispersion in water. Additionally, to confirm the importance of the carbene generation for promoting ligand coordination on the gold surfaces, we have conducted a control experiment, where ligand exchange was carried out using APEIm-ium-PIMA-PEG (i.e., in the absence of KOtBu). Results showed that ligation and phase transfer could ultimately take place. However, the resulting AuNPs exhibited poor colloidal stability in DI water, as color change and red shift in the SPR were observed (see Supporting Information, Figure S2). This implies that the presence of KOtBu as a strong base is critical for forming the carbene groups, which drives coordination onto the AuNPs.

For the ex situ route, an aliquot of OLA-AuNP stock dispersion was subjected to one round of precipitation (to remove excess free ligands), and the pellet was redispersed in $CHCl_3$, mixed with preformed NHC-PIMA-PEG, and then left to react while stirring overnight at room temperature; the molar excess ligand was varied between 5000- and 15,000-fold. The new NHC polymer-coated NPs were purified by applying two rounds of precipitation using excess hexane, yielding a pellet of NHC-PIMA-PEG-stabilized AuNPs. After drying under the nitrogen flow, the pellet was dispersed in water, and the hydrophilic dispersion was purified from excess ligands and solubilized OLA using a membrane filtration device, as described above.

Characterization of the NHC-Capped AuNPs. Characterization of the AuNPs following ligation with various new compounds was carried out using: (1) ^{1}H NMR spectroscopy, (2) UV−vis absorption spectroscopy, (3) DLS, and (4) TEM, and data were compared side by side with results acquired from the starting hydrophobic OLA-AuNPs. These measurements allowed us to assess the quality of the NPs stabilized with the new ligands presenting NHC-coordinating groups.

^{1}H NMR Characterization. The measurements were applied to the ligand precursor (before base treatment) and after carbene transformation, when the base treatment was carried out prior to ligand exchange (ex situ). Alternatively, when carbene generation was carried out in situ, the NMR data collected from the ligand precursor alone were compared to the spectra from the NHC ligand coordinated onto the NPs after KOtBu treatment. Characterization of the first monomer ligand was limited to NHC-APE and its precursor APEIm-ium. As the dispersion of NHC-APE-AuNPs exhibited poor stability, our experiments were mainly aimed at verifying the carbene generation following base treatment. The spectra collected before (top spectrum) and immediately after (bottom spectrum) reaction with KOtBu show that all the proton peaks along with the corresponding integrals expected for the compounds have been measured (see Figure 3a). More precisely, the spectrum acquired from APEIm-ium shows a singlet peak at 7.55 ppm attributed to the merged two protons (i, j) along with a peak at 8.86 ppm ascribed to the C2-proton (h) in the imidazole ring. The acquired spectrum after KOtBu treatment shows that the peak at 7.55 ppm was preserved, while the one at 8.86 ppm (h) disappeared. This provides evidence for carbene formation, which is consistent with the anticipated structure of the NHC-APE ligand.

When APEIm-ium conversion to NHC for the two PEGylated compounds (PEG-EIm-ium and APEIm-ium-PIMA-PEG) was carried out in situ, the ^{1}H NMR data acquired from the precursor compounds were compared side by side with those collected from the NHC-ligated AuNPs dispersed in D_2O, which provided further confirmation that coordination onto the AuNPs was promoted by the in situ generated NHC groups. Figure 3b,c shows representative ^{1}H NMR spectra collected from solutions of the ligand precursors only, namely, PEG-EIm-ium and APEIm-ium-PIMA-PEG (see top spectra in panels 3b,c) side by side with the corresponding surface-ligated NHC-PEG- and NHC-PIMA-PEG-AuNPs after phase transfer to D_2O (see bottom spectra in panels 3b,c). The spectra acquired from solutions of the pure ligands, PEG-EIm-ium or APEIm-ium-PIMA-PEG, show two distinct peaks: one assigned to the merged ring protons (i and j), measured at 7.55 (for PEG-EIm-ium) or at 7.59 ppm (for APEIm-ium-PIMA-PEG), and another assigned to the C2-proton (h), measured at 8.76 ppm (for PEG-EIm-ium) or at 8.87 ppm for (APEIm-ium-PIMA-PEG). The NMR data were also used to estimate the ligand stoichiometry. The spectrum of PEG-EIm-ium (panel 3b, top) shows peaks at

https://dx.doi.org/10.1021/acs.chemmater.0c03918
Chem. Mater. 2021, 33, 921−933

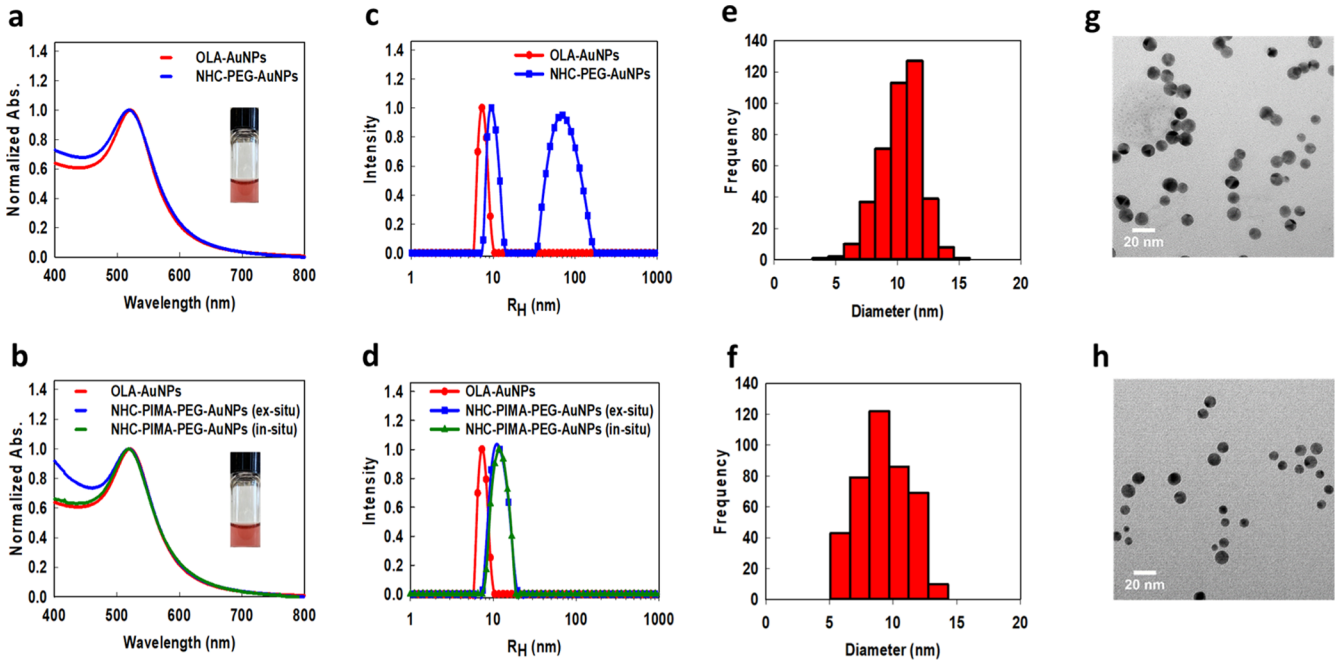

Figure 4. (a,b) Side-by-side UV−vis spectra collected from OLA-AuNPs (before, red lines) and after ligand substitution with NHC-PEG or NHC-PIMA-PEG (ex situ, blue line and in situ, green line). Insets show white light images of dispersions of the newly coated AuNPs in water. (c,d) Histograms of the intensity vs hydrodynamic radius measured for the NHC-PEG-AuNPs or NHC-PIMA-PEG-AuNPs (ex situ, blue line and in situ, green line) plotted together with the one measured before ligand exchange (red line). (e,f) Size distribution histograms extracted from the TEM imaging data measured for NHC-PEG-AuNPs and NHC-PIMA-PEG-AuNPs shown in panels (g,h): NHC-PEG-AuNPs (diameter ∼ 10.2 ± 1.7 nm) and NHC-PIMA-PEG-AuNPs (diameter ∼ 9.2 ± 1.9 nm).

3.32 ppm and 3.62 ppm, ascribed to the methyl and ethylene glycol protons of the PEG-OCH_3 moieties, respectively, along with a peak at 1.5 ppm ascribed to the methyl (u) protons in the terminal EIm-ium salt. Similarly, the spectrum acquired from the polymer (panel 3c, top) also proves that both imidazolium salt and PEG moieties have been installed along the PIMA chain for APEIm-ium-PIMA-PEG. These data were further exploited to extract a measure for the number of PEG blocks and imidazolium salt groups along the PIMA chain by comparing the integrated peaks of the methoxy at 3.41 ppm and the terminal methyl of the imidazolium salt (at 1.5 ppm) to that of the methyl groups in the PIMA chain (broad peak at 1.0 ppm). We estimate that the molar ratio of APEIm-ium/PEG per polymer is ∼50:50. The data collected from the AuNP dispersions show that only the acidic proton (h) peak is conspicuously absent from the two sets of NHC-ligated AuNP dispersions (NHC-PEG and NHC-polymer); see bottom spectra in Figure 3b,c. We should also note that the ^{1}H NMR spectra from the AuNP dispersions indicate that OLA was completely removed from the AuNP surfaces because the characteristic peak around 5.3 ppm (ascribed to, i.e., −C$\underline{H}_2$═C$\underline{H}_2$−) is absent.[64] Finally, we note that the spectra acquired from the newly coated AuNPs exhibit peak broadening due to coordination of the NHC ligands onto the surface of AuNPs, which is a common feature of NP-bound ligands.[65] These combined data provide strong evidence that base treatment promotes the generation of carbene species, which in turn competitively displace the native cap, ultimately proving that coordination of the new ligands is driven by carbene-to-Au bonding.

Optical Characterization. Figure 4a,b shows representative absorption spectra collected from AuNP dispersions before and after ligand exchange with NHC-PEG and NHC-PIMA-PEG. The absorption spectra collected from the NHC-PEG- and NHC-PIMA-PEG-capped AuNPs (blue profiles) are nearly identical to those measured for OLA-AuNP dispersions in hexane (red profiles), with SPR band located at ∼520 nm for all dispersions. The identical optical properties before and after ligand substitution indicate that the present surface functionalization using NHC-based ligands preserves the integrity of the gold nanocolloids.

Dynamic Light Scattering. DLS measurements exploit the time-dependent intensity scattered from fluid dispersions to extract values for the AuNP hydrodynamic size (from the diffusion coefficient data) under different conditions, namely, from dispersions of the as-prepared (OLA-coated) AuNPs and dispersions of AuNPs after ligand substitution with NHC-PEG (under in situ conditions), or with NHC-PIMA-PEG (under both in situ and ex situ conditions). In addition, given the fact that DLS exploits the Rayleigh laser scattered intensity from the solute objects (which strongly depends on size, Int. ∼ R^6), it is naturally suited for probing thermodynamic stability of the colloids. In particular, DLS can ultimately identify NP aggregate formation in the dispersions for ligands that do not promote repulsive stabilizing interactions. Figure 4c,d shows representative histograms of the scattered intensity versus hydrodynamic radius (Int. vs R_H), extracted from the Laplace Transform of the autocorrelation function (see Supporting Information for additional details about DLS). The abovementioned histograms indicate that homogeneous samples (with a single peak profile) characterize dispersions of the native OLA-AuNPs in hexane (R_H ∼ 7.6 nm) and of NHC-PIMA-PEG-AuNPs in water (R_H ∼ 11 nm), regardless of the ligand substitution route used, namely, using in situ or ex situ conditions. However, the histogram acquired from the data for NHC-PEG-AuNPs shows that two populations of scattering objects are present: a narrow one

https://dx.doi.org/10.1021/acs.chemmater.0c03918
Chem. Mater. 2021, 33, 921−933

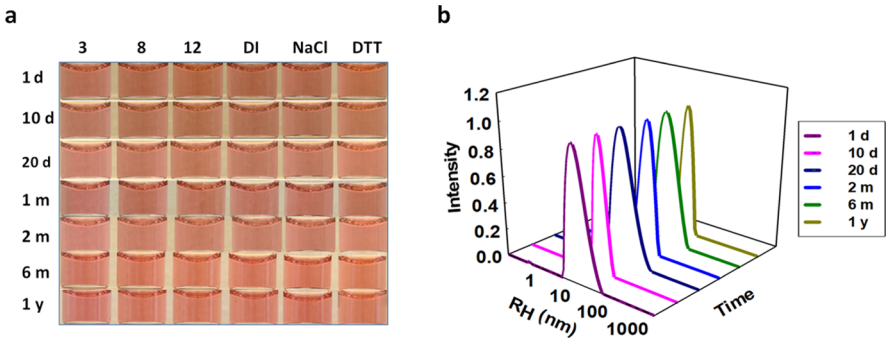

Figure 5. Colloidal stability tests: (a) AuNPs ligand exchanged with NHC-PIMA-PEG dispersed in phosphate buffer (20 mM) over the pH 3, 8, and 12, in DI water, in the presence of 1 M NaCl and 0.1 M DTT. (b) Time progression of the hydrodynamic radius measured from NHC-PIMA-PEG-AuNP dispersions in DI water.

corresponding to smaller colloids (single NPs, with $R_H \sim 9.5$ nm) and another of small aggregates (with $R_H \sim 68$ nm). The fraction of aggregates is rather small compared to that of single NPs, with <1% (based on the number weighted data) of the total number of scattering objects being aggregates. Nonetheless, the dispersions appeared clear with no precipitate buildup even after several months of storage (additional data are available in the Supporting Information). The larger R_H values measured for the NHC-coated AuNPs compared to the starting OLA-AuNPs reflect an increase in the contribution of hydrodynamic interactions to the Brownian motion measured for the nanocolloids when the coating is changed from OLA to NHC-PEG or NHC-PIMA-PEG. Those contributions are highest for NHC-polymer coating ($R_H \sim 11$ nm), reflecting the multi-coordinating nature and spatial extension of the polymer coating. The absence of a second population with a larger size in the NHC-PIMA-PEG-AuNPs further proves that the higher coordination provided by the polymer coating imparts steric stability to the nanocolloids and prevents aggregate formation. In comparison, the monomer coating imparts moderate steric stabilization of the NPs, which manifests in the appearance of a fraction of small aggregates in the sample.

Transmission Electron Microscopy. Analysis of the TEM images collected from OLA-AuNPs shows that these NPs are spherical in shape with an average diameter of 9.5 ± 1.5 nm, and substitution of the OLA coat with the NHC-modified ligands yielded spherical NPs with a diameter of ∼10.2 ± 1.7 nm for NHC-PEG-AuNPs and ∼9.2 ± 1.9 nm for NHC-PIMA-PEG-AuNPs; see TEM micrographs shown in Figure 4g,h. The histograms of the size distribution illustrated in Figure 4e,f were extracted directly from the TEM micrographs, and sizes were averaged over ∼400 NPs. These results clearly indicate that cap exchange with both sets of ligands essentially maintained the size and shape of the colloids, without significant etching of the AuNP cores under the conditions used.

Colloidal Stability Tests. The colloidal stability tests were limited to aqueous dispersions of AuNPs capped with NHC-PEG and NHC-PIMA-PEG ligands (i.e., prepared via ex situ carbene generation) and carried out under several biologically relevant conditions. These include dispersions in phosphate buffers over the pH range of 3−12 in DI water, in high salt solutions (1 M NaCl), and in the presence of a reducing compound (DTT, 0.1 M). Figure 5a shows white light images of NHC-PIMA-PEG-AuNP dispersions in buffer media tracked over a period of 1 year. Data indicate that AuNPs ligated with the NHC polymer remained stable without any sign of degradation or aggregation buildup over the entire set of conditions probed for at least 1 year of storage. The hydrodynamic size of the NHC-polymer-AuNPs in DI water was tracked during storage using DLS measurements. The histograms shown in Figure 5b indicate that the radius measured for NHC-PIMA-PEG-AuNPs remained constant (R_H ∼11 nm) throughout the full storage period. It should also be noted that R_H remained constant (∼11 nm) over the pH range in the presence of 1 M NaCl or 0.1 M DTT (data not shown). In comparison, even though dispersions of NHC-PEG-capped AuNPs were stable over the pH range 3−12, and in 1 M NaCl for 1 year, the dispersions in 0.1 M DTT exhibited slight color change to bluish after ∼1 week (see Supporting Information, Figure S3). Similarly, the intensity versus R_H histograms collected from the NHC-PEG-AuNP dispersions in DI water or 1 M NaCl consistently showed a bimodal distribution, while staying visually homogeneous throughout the test period, indicating the persistent presence of a small fraction of aggregates, as shown in Figure S3b.

However, testing the dispersion stability in the presence of DTT is more complex. Being molecular-scale and presenting two thiols in their structure, DTT molecules can easily diffuse through the surface coating of Au and other nanocolloids and competitively displace weakly bound ligands.[66] Such competition becomes more effective in the presence of added NaCl promoted by counterion screening effects.[66,67] This alters the surface coating of AuNPs, causing progressive aggregation with time; a coating relying on DTT alone does not provide enough steric repulsions between the NPs to impart colloidal stability. We have provided data on the DTT test applied to the newly capped AuNP dispersions below.

DTT Competition Tests. Here, we apply this routine test to gauge the strength of the coordination interactions between NHC-modified ligands and AuNPs using competition from excess DTT in the presence of added NaCl. Competitive displacement of surface ligands by DTT alters the spectroscopic properties of AuNPs, manifesting in a time-dependent broadening of the SPR band and reduction in its peak intensity, combined with increase in the absorbance at longer wavelength; a visual change in the dispersion color also takes place.[66] To quantify these changes, we use an aggregation factor (AF), which is defined as the ratio between optical densities near the baseline (here at ∼714 nm) and at ∼520 nm (the SPR value).[66] As defined, the AF should either remain unaltered or exhibit minor and slow change with time if the ligands are strongly bound to the Au surfaces. Conversely, if affinity to the colloids is weak and the ligands can be easily displaced by DTT, the AuNP dispersion becomes unstable, resulting in progressive increase in the AF with time.

https://dx.doi.org/10.1021/acs.chemmater.0c03918
Chem. Mater. 2021, 33, 921−933

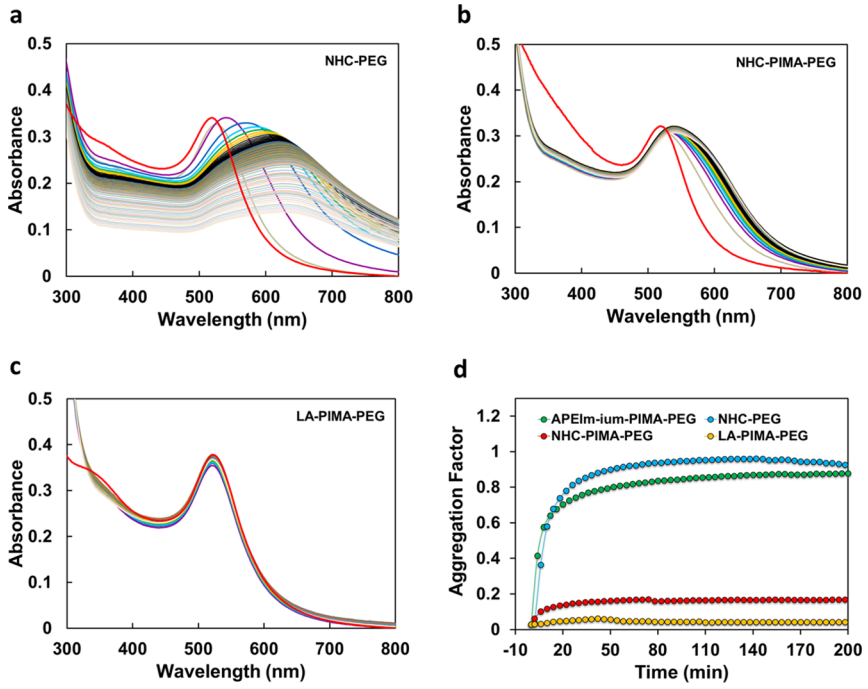

Figure 6. DTT competition tests. Time progression of UV−vis absorption spectra collected from AuNPs capped with (a) NHC-PEG (in situ), (b) NHC-PIMA-PEG (ex situ, 10,000-fold), and (c) LA-PIMA-PEG. (d) Normalized AF extracted from the absorption data shown in panels (a−c) and data shown in the Supporting Information (Figure S4). The AF profiles in panel (d) are from AuNPs coated with NHC-PEG (in situ, blue circles), APEIm-ium-PIMA-PEG (green circles), NHC-PIMA-PEG (ex situ and 10,000-fold, red circles), and LA-PIMA-PEG (orange circles).

We tracked the progression of the UV−vis absorption spectra collected from dispersions of AuNPs (containing 0.1 M DTT and 400 mM NaCl), which are surface-stabilized with NHC-PEG (NHC-monomer), NHC-PIMA-PEG (NHC-polymer), and APEIm-ium-PIMA-PEG, along with a coating made of LA-PIMA-PEG (a multi lipoic acid- and PEG-modified PIMA polymer, with a molar stoichiometry LA/PEG = 50:50, similar to that of the NHC-PIMA-PEG polymer), as shown in Figure 6. Ligand substitution with LA-PIMA-PEG was carried out using incubation of OLA-AuNPs with excess ligands for ∼18 h; this high affinity coating provides a well-established control system.[50,68] The polymer synthesis and purification of LA-PIMA-PEG were reported in our previous works.[50,52] The test was extended over a period of ∼3 h. Representative spectra collected from dispersions of the AuNP cap exchanged with the various NHC ligands are shown in the Supporting Information (Figure S4). The corresponding AF versus time profiles for all sets of dispersions are compiled in Figures 6d and S4. Clearly, the data show a wide range of patterns for the progression of the absorption spectra with time depending on the ligand structure and the substitution conditions used. Data show that the most pronounced changes are measured for dispersions with the following AuNP-ligand combinations: APEIm-ium-PIMA-PEG-AuNPs (unmodified polysalt ligand) and NHC-PEG-AuNPs (monomer). For these dispersions, we observe a progressive color change from red to violet combined with turbidity buildup, indicating aggregate formation in the samples, which can yield macroscopic sedimentation in the worst cases. In comparison, data collected from NHC-PIMA-PEG-AuNPs (multi-NHC polymer) show slower change in the spectra with time, even though the exact profiles vary widely depending on factors such as in situ versus ex situ conditions, excess ligand concentration used, temperature, increase in pH (base concentration), and incubation time; all these factors can affect the DTT test results; see Supporting Information, Figure S4. The data in Figure 6d also show that compared to AuNPs capped with the various NHC-modified ligands, the AF profile acquired for LA-PIMA-PEG-AuNPs is essentially flat and close to the baseline. This clearly indicates that substituting OLA with LA-PIMA-PEG yields dispersions with much stronger resistance to DTT destabilization.[50]

We now discuss the abovementioned findings in comparison to prior studies, where surface binding driven by NHC coordination onto Au nanocolloids has been investigated. Overall, our results clearly prove that ligation onto AuNPs promoted by NHC-to-Au coordination can be easily implemented, and if the ligands are further modified to present hydrophilic moieties, this strategy yields water-dispersible nanocolloids. Additionally, we found that installing several NHC groups along a polymer chain yields a multicoordinating ligand that can impart long-term stability in buffer media over a wide pH range, and in the presence of high salt concentration or DTT reducing agent that extend to at least 1 year of storage. Our results expand on the ideas reported by Johnson and co-workers and demonstrate that being a soft Lewis base, carbene can strongly interact with Au nanocolloid surfaces, which have a soft Lewis acidic character.[69] The Johnson group subsequently showed that appending a PEG block onto the NHC moiety imparts additional flexibility by allowing the growth of hydrophilic AuNPs, starting from the PEG-NHC-Au(I) complex as a precursor.[46] Our strategy for preparing the PEGylated mono-NHC provides an alternative pathway for designing hydrophilic carbene-stabilized AuNPs via ligand substitution starting with OLA-AuNPs. The NHC-PEG-stabilized AuNPs exhibit good long-term colloidal stability (i.e., several months of storage), which agrees with the data reported by Johnson's group. We should note that their tests were limited to a period of up to 3 months and used slightly

https://dx.doi.org/10.1021/acs.chemmater.0c03918
Chem. Mater. 2021, 33, 921−933

longer PEG blocks. Nonetheless, our DLS data still indicate the presence of persistent small aggregates, which are not easily identified using absorption measurements, TEM data, or visual inspection, as done in some of the previous reports. More precisely, our DLS data allowed for identifying the presence of a small fraction of rather stable aggregates made of ∼45−47 AuNPs (if we assume a close-packed arrangement of the NPs in those aggregates), which persist for several months, yet without affecting the dispersion appearance or the UV−vis absorption properties. Though promising, monodentate NHC ligands are not able to impart long-term stabilization, a result that has also been observed for other inorganic nanocolloids surface-coated with a variety of monodentate ligands.[70] In comparison, the PEGylated multi-NHC polymers provide enhanced coordination affinity onto AuNPs, manifesting in the complete displacement of the native cap. It also yields dispersions that are colloidally stable and free of aggregates over a wide range of conditions and for an extended period (see Figure 5). These data agree with previous findings reported by Crudden and co-workers, who showed that bidentate NHC-modified ligands provide enhanced stability to AuNP dispersed in organic media.[71] Mixed NHC- and thiol-bidentate interactions were tested by the groups of Glorius and Johnson to improve the effectiveness of the NHC-coating strategy applied to Pd NPs and Au nanorods.[40,72] We should stress that our long-term stability results for the PEGylated monomer and polymer ligands provide further proof that the NHC-Au bonding once formed is stable even in aqueous media. Additionally, the bonding stability is observed for samples prepared via in situ carbene generation in the presence of AuNPs as well as ex situ carbene generation (where NHC groups are generated before mixing with the NPs).

Nonetheless, the colloidal stability data as evaluated using the DTT competition test reveal that multi-NHC coordination onto Au surfaces is weaker than the one involving the conventional multi-thiol ligands. The comparison should be considered, while keeping in mind that the net number of thiol-coordinating groups in LA-PIMA-PEG ligands is higher because each LA would yield two coordinating groups, implying that there are approx. 2× thiols than NHCs per polymer.[68] However, this finding should be discussed using other features specific to NHC-Au binding. Recent work by He and co-workers compared the grafting density of two sets of monodentate polymer ligands, one presenting a terminal thiol and the other an NHC group. A solution of each polymer with the same concentration was flowed over an Au surface while tracking changes in the SPR signature, which provided estimates for the apparent binding constant K_a for both ligands. They reported that the binding constant of the thiol polymer is approximately 1 order of magnitude larger than that of the NHC polymer, reflecting a larger grafting density of thiol groups on the Au surface and thus a lower K_{off} rate for this polymer ligand.[73] We would like to note that the lower grafting density of the NHC polymer cannot be simply attributed to the steric hindrance of the carbene moieties because the larger spatial extension of the polymer coils (due to entropy consideration and excluded volume effects) will mitigate these effects.

After careful examination of our data and analysis of the existing literature, we would like to propose a rationale that can explain the rather strong difference in the DTT test results, as shown in Figure 6 as well as in the results reported by He and co-workers.[73] Interactions between NHC groups and Au atoms are predicted to be very strong because they involve soft-to-soft Lewis base−acid interactions and the sharing of two electrons. These have led some reports to view the NHC-to-Au(0) bond as covalent.[74] One can thus assume that NHC-to-Au(0) binding is stronger than that governing the covalent Au(0)−Au(0) interactions. This disturbs the arrangements of the NHC-bound gold atoms near the surface, leading to the classification of NHC-Au as an adatom rather than an integral part of the crystalline lattice.[75] This process can eventually "dislodge" NHC-bound Au as complexes in the dispersions, which can be detected by mass spectrometry, for example. These events will reduce the surface ligand density on the nanocolloids,[29,76,77] yielding weaker resistance to competition from DTT. These factors combined together may be the source for the lower stability exhibited by NHC-PIMA-PEG-protected AuNPs compared to those stabilized with LA-PIMA-PEG, as shown in our DTT competition test. They may also be the cause for the wide range of DTT stability profiles shown for the NHC-PIMA-PEG-AuNPs prepared under varying conditions, as shown in Figures 6 and S4.

This rationale is consistent with results reported by Johnson's group, where bidentate thiol-NHC-Au(I) complexes were shown to better coordinate onto the surfaces of Au nanorods by first allowing the thiol to initiate surface binding via thiol-to-Au coordination, followed by reduction of the NHC-Au(I) complex to NHC-Au(0) under mild conditions.[72] The NHC-Au(I) complex is thus added to the nanorod surface as an adatom, preventing the reorganization of the underlying surface lattice, which can occur for NHC-Au(0) binding.[72] This model is supported by preliminary data collected in our laboratory relying on MALDI-MS spectrometry, where the presence of surface-released soluble NHC-PEG-Au(I) complexes was observed after the ligand exchange and purification steps. We are in the process of performing a set of coordinated experiments combining mass spectrometry and X-ray photoelectron spectroscopy to develop a complete picture of the nature of the interactions between NHC groups and Au nanocolloids. We hope to report on those results in a future publication.

CONCLUSIONS

We have designed a new set of NHC-based metal-coordinating compounds starting with simple imidazole ring structures and tested them as ligands for the stabilization of AuNPs. We first showed that NHC-modified ligands promote rapid coordination onto AuNP colloids. When the NHC-ligand was appended with the PEG hydrophilic block, this coating yielded NPs that are readily dispersible in buffer media, but stability was rather limited. However, when several NHC groups and PEG blocks were installed along a polymer structure by, for example, relying on the one-step nucleophilic addition reaction using PIMA, the resulting multidentate NHC-coating provided aqueous AuNP dispersions that were free of aggregates and colloidally stable under various conditions for at least 1 year. We further exploited the DTT stability data collected from AuNP dispersions with either NHC or thiol-based ligands to propose a rationale for how NHC binding onto the NP surfaces affects the resistance to competition from reducing small molecules. The carbene-driven coordination onto AuNPs was confirmed using ^{1}H NMR spectroscopy. These results are highly promising, as they expand and complement prior findings, which have discussed the ability of this Lewis base group to strongly interact with AuNP surfaces. We anticipate that such NHC-based coordinating ligands would be ideally suitable for the surface coating of other transition metal core colloids, considering that these materials tend to present surfaces with the soft Lewis acid nature, such as

https://dx.doi.org/10.1021/acs.chemmater.0c03918
Chem. Mater. 2021, 33, 921−933

semiconductor colloidal nanocrystals (QDs). Because these nanocrystals exhibit unique photophysical properties, their absorption and fluorescent properties can be affected by the structure of the NHC coating used.[78,79] As such, NHC-based ligands will be highly suitable for stabilizing an array of inorganic colloids and for potential use in applications ranging from drug delivery and biomedicine to catalysis.

EXPERIMENTAL SECTION

The experimental section will be limited to detailing the ligand exchange steps applied using mono- and multidentate NHC ligands, and starting with OLA-capped AuNPs, along with the NMR sample preparation and DTT stability tests. Synthesis of the various ligands, namely, NHC-APE, NHC-PEG, and NHC-PIMA-PEG is detailed in the Supporting Information.

Ligand Exchange. *In Situ Preparation of NHC-PEG-Capped AuNPs.* Typically, an OLA-AuNP dispersion in hexane (225 μL, 0.67 μM) was precipitated using excess EtOH and redispersed in THF (400 μL). Separately, PEG-EIm-ium salt (41 mg) was dissolved in THF (400 μL) at an excess molar concentration with respect to the NPs of ~300,000. The AuNP dispersion and ligand solution were then mixed in a vial forming a homogeneous phase. The vial was sealed with a rubber septum and subjected to 3−4 round of vacuum, followed by purging with N_2 in order to switch the atmosphere in the vial to nitrogen. KOtBu (10 mg) dissolved in 500 μL of dried THF was added dropwise while stirring, and the mixture was then left to stir at 40 °C overnight. This step promotes the transformation of imidazolium to NHC. The NHC-PEG-capped AuNPs were precipitated by adding excess hexane, sonicated for ~1 min, and then centrifuged at 3500 rpm for 2 min, followed by removal of the supernatant. This procedure was repeated one more time. The precipitate containing NHC-PEG-AuNPs was gently dried under a nitrogen flow and then dispersed in DI water. The hydrophilic dispersion of NHC-PEG-AuNPs was purified from excess ligands by applying two rounds of concentration/dilution using a membrane centrifugal filtration device (Amicon Ultra, 50 kDa).

In Situ Ligand Exchange of OLA-AuNPs with NHC-PIMA-PEG. Hydrophobic OLA-AuNP dispersions (75 μL, 0.67 μM) in hexane were precipitated using excess EtOH and redispersed in THF (400 μL). Separately, APEIm-ium-PIMA-PEG salt (19 mg) was dissolved in THF (400 μL) at an excess molar concentration (~15,000) with respect to AuNPs. The AuNP dispersion and ligand solution were then mixed in a vial yielding a homogeneous phase. The vial was sealed with a rubber septum, and the mixture was purged multiple times (3−4) with N_2, as done above. KOtBu (3 mg) dissolved in dried THF (600 μL) was added dropwise while stirring, and the mixture was left stirring at 40 °C overnight. The NHC-PIMA-PEG-capped AuNPs were precipitated by adding an excess amount of hexane. Following sonication for ~1 min, the solution was centrifuged (at 3500 rpm, 2 min), and the supernatant was discarded. The pellet containing NHC-PIMA-PEG-AuNPs was gently dried under nitrogen flow and then readily dispersed in DI water. Finally, two rounds of concentration/dilution using a membrane centrifugal filtration device (Amicon Ultra, 50 kDa) were applied to discard excess free ligands.

Ex Situ Ligand Exchange of OLA-AuNPs with NHC-PIMA-PEG. Ethanol was added to OLA-AuNP stock solution (400 μL, 0.178 μM) in a 7 mL scintillation vial to precipitate the NPs, and the mixture was centrifuged (at 3700 rpm for 5 min). The supernatant containing excess free OLA ligands was discarded; then, the pellet was dispersed in $CHCl_3$ (300 μL) and mixed with NHC-PIMA-PEG (20 mg). The reaction mixture was stirred overnight at room temperature. Then, excess hexane was added to precipitate the polymer-capped AuNPs. The supernatant was decanted; then another round of precipitation was carried out by adding $CHCl_3$ and excess hexane. After discarding the supernatant, the pellet was dried under a nitrogen flow and then dispersed in DI water. The aqueous AuNP dispersion was filtered using a 0.45 μm syringe filter, followed by two rounds of purification using a membrane filtration device, as described above.

NMR Sample Preparation. Because ^{1}H NMR spectra were collected from dispersions in the deuterated solvent, transfer to D_2O was carried out during the final purification step by applying 3−4 rounds of concentration/dilution using deuterium oxide instead of water. Approx. 500 μL of NHC-capped AuNPs in D_2O was collected and used for acquiring the ^{1}H NMR spectra. Pulsed-field gradient-based water suppression was applied to all data collected in D_2O.

DTT Stability Test. In a typical sample preparation, DTT solution (15 μL, 4 M) was mixed with NaCl solution (80 μL, 3 M) in a quartz cuvette (0.5 cm × 0.5 cm) and further diluted with DI water before addition of the desired volume of AuNP dispersions. The dispersion was then rapidly added to the DTT/NaCl solution and mixed thoroughly. The total volume of the dispersion was adjusted to 600 μL, and the final concentrations of AuNPs, DTT, and NaCl were 10.6 nM, 0.1 M, and 400 mM, respectively. For each sample, absorption spectra were collected every 2 min for a total of 200 min.

ASSOCIATED CONTENT

Supporting Information

The Supporting Information is available free of charge at https://pubs.acs.org/doi/10.1021/acs.chemmater.0c03918.

Materials, instrumentation, ligand synthesis, ligand exchange, characterization data, colloidal stability tests, UV−vis absorption spectra, and DTT competition tests (PDF)

AUTHOR INFORMATION

Corresponding Author

Hedi Mattoussi − *Department of Chemistry and Biochemistry, Florida State University, Tallahassee, Florida 32306, United States;* orcid.org/0000-0002-6511-9323; Email: mattoussi@chem.fsu.edu

Authors

Neda Arabzadeh Nosratabad − *Department of Chemistry and Biochemistry, Florida State University, Tallahassee, Florida 32306, United States*

Zhicheng Jin − *Department of Chemistry and Biochemistry, Florida State University, Tallahassee, Florida 32306, United States*

Liang Du − *Department of Chemistry and Biochemistry, Florida State University, Tallahassee, Florida 32306, United States*

Mannat Thakur − *Department of Chemistry and Biochemistry, Florida State University, Tallahassee, Florida 32306, United States*

Complete contact information is available at: https://pubs.acs.org/10.1021/acs.chemmater.0c03918

Notes

The authors declare no competing financial interest.

ACKNOWLEDGMENTS

We thank FSU and the National Science Foundation (NSF-CHE #1508501 and #2005079), AFOSR (grant no. FA9550-18-1-0144), and Kasei-Asahi for financial support. We also thank Banghao Chen, Chengqi Zhang, Sisi Wang, and Yan Xin for help with the TEM and NMR experiments and for the fruitful discussions. The TEM work was performed at the National High Magnetic Field Laboratory, which is supported by National Science Foundation Cooperative agreement no. DMR-1644779 and the State of Florida.

REFERENCES

(1) Dulkeith, E.; Morteani, A. C.; Niedereichholz, T.; Klar, T. A.; Feldmann, J.; Levi, S. A.; van Veggel, F. C. J. M.; Reinhoudt, D. N.; Möller, M.; Gittins, D. I. Fluorescence Quenching of Dye Molecules

near Gold Nanoparticles: Radiative and Nonradiative Effects. *Phys. Rev. Lett.* **2002**, *89*, 203002.
(2) Daniel, M.-C.; Astruc, D. Gold nanoparticles: Assembly, supramolecular chemistry, quantum-size-related properties, and applications toward biology, catalysis, and nanotechnology. *Chem. Rev.* **2004**, *104*, 293−346.
(3) Singh, M. P.; Strouse, G. F. Involvement of the LSPR Spectral Overlap for Energy Transfer between a Dye and Au Nanoparticle. *J. Am. Chem. Soc.* **2010**, *132*, 9383−9391.
(4) Acuna, G. P.; Bucher, M.; Stein, I. H.; Steinhauer, C.; Kuzyk, A.; Holzmeister, P.; Schreiber, R.; Moroz, A.; Stefani, F. D.; Liedl, T.; Simmel, F. C.; Tinnefeld, P. Distance Dependence of Single-Fluorophore Quenching by Gold Nanoparticles Studied on DNA Origami. *ACS Nano* **2012**, *6*, 3189−3195.
(5) Aldeek, F.; Safi, M.; Zhan, N.; Palui, G.; Mattoussi, H. Understanding the Self-Assembly of Proteins onto Gold Nanoparticles and Quantum Dots Driven by Metal-Histidine Coordination. *ACS Nano* **2013**, *7*, 10197−10210.
(6) Kapur, A.; Aldeek, F.; Ji, X.; Safi, M.; Wang, W.; Del Cid, A.; Steinbock, O.; Mattoussi, H. Self-Assembled Gold Nanoparticle-Fluorescent Protein Conjugates as Platforms for Sensing Thiolate Compounds via Modulation of Energy Transfer Quenching. *Bioconjugate Chem.* **2017**, *28*, 678−687.
(7) Abadeer, N. S.; Brennan, M. R.; Wilson, W. L.; Murphy, C. J. Distance and Plasmon Wavelength Dependent Fluorescence of Molecules Bound to Silica-Coated Gold Nanorods. *ACS Nano* **2014**, *8*, 8392−8406.
(8) Gong, S.-H.; Kim, J.-H.; Ko, Y.-H.; Rodriguez, C.; Shin, J.; Lee, Y.-H.; Dang, L. S.; Zhang, X.; Cho, Y.-H. Self-aligned deterministic coupling of single quantum emitter to nanofocused plasmonic modes. *Proc. Natl. Acad. Sci. U.S.A.* **2015**, *112*, 5280−5285.
(9) Jain, P. K.; Huang, X.; El-Sayed, I. H.; El-Sayed, M. A. Review of some interesting surface plasmon resonance-enhanced properties of noble metal nanoparticles and their applications to biosystems. *Plasmonics* **2007**, *2*, 107−118.
(10) Bodelón, G.; Montes-García, V.; López-Puente, V.; Hill, E. H.; Hamon, C.; Sanz-Ortiz, M. N.; Rodal-Cedeira, S.; Costas, C.; Celiksoy, S.; Pérez-Juste, I.; et al. Detection and imaging of quorum sensing in Pseudomonas aeruginosa biofilm communities by surface-enhanced resonance Raman scattering. *Nat. Mater.* **2016**, *15*, 1203−1211.
(11) Langer, J.; Jimenez de Aberasturi, D.; Aizpurua, J.; Alvarez-Puebla, R. A.; Auguié, B.; Baumberg, J. J.; Bazan, G. C.; Bell, S. E. J.; Boisen, A.; Brolo, A.G.; et al. Present and Future of Surface-Enhanced Raman Scattering. *ACS Nano* **2020**, *14*, 28−117.
(12) Hamad-Schifferli, K.; Schwartz, J. J.; Santos, A. T.; Zhang, S.; Jacobson, J. M. Remote electronic control of DNA hybridization through inductive coupling to an attached metal nanocrystal antenna. *Nature* **2002**, *415*, 152−155.
(13) Howes, P. D.; Chandrawati, R.; Stevens, M. M. Colloidal nanoparticles as advanced biological sensors. *Science* **2014**, *346*, 1247390.
(14) Lim, E.-K.; Kim, T.; Paik, S.; Haam, S.; Huh, Y.-M.; Lee, K. Nanomaterials for Theranostics: Recent Advances and Future Challenges. *Chem. Rev.* **2015**, *115*, 327−394.
(15) Saha, K.; Agasti, S. S.; Kim, C.; Li, X.; Rotello, V. M. Gold Nanoparticles in Chemical and Biological Sensing. *Chem. Rev.* **2012**, *112*, 2739−2779.
(16) Dreaden, E. C.; Alkilany, A. M.; Huang, X.; Murphy, C. J.; El-Sayed, M. A. The golden age: gold nanoparticles for biomedicine. *Chem. Soc. Rev.* **2012**, *41*, 2740−2779.
(17) Li, K.; Liu, B. Polymer-encapsulated organic nanoparticles for fluorescence and photoacoustic imaging. *Chem. Soc. Rev.* **2014**, *43*, 6570−6597.
(18) Zhan, N.; Palui, G.; Safi, M.; Ji, X.; Mattoussi, H. Multidentate Zwitterionic Ligands Provide Compact and Highly Biocompatible Quantum Dots. *J. Am. Chem. Soc.* **2013**, *135*, 13786−13795.
(19) García, I.; Sánchez-Iglesias, A.; Henriksen-Lacey, M.; Grzelczak, M.; Penadés, S.; Liz-Marzán, L. M. Glycans as biofunctional ligands for gold nanorods: stability and targeting in protein-rich media. *J. Am. Chem. Soc.* **2015**, *137*, 3686−3692.
(20) Lavrich, D. J.; Wetterer, S. M.; Bernasek, S. L.; Scoles, G. Physisorption and Chemisorption of Alkanethiols and Alkyl Sulfides on Au(111). *J. Phys. Chem. B* **1998**, *102*, 3456−3465.
(21) Crudden, C. M.; Horton, J. H.; Ebralidze, I. I.; Zenkina, O. V.; McLean, A. B.; Drevniok, B.; She, Z.; Kraatz, H.-B.; Mosey, N. J.; Seki, T.; Keske, E. C.; Leake, J. D.; Rousina-Webb, A.; Wu, G. Ultra stable self-assembled monolayers of N-heterocyclic carbenes on gold. *Nat. Chem.* **2014**, *6*, 409−414.
(22) Crudden, C. M.; Horton, J. H.; Narouz, M. R.; Li, Z.; Smith, C. A.; Munro, K.; Baddeley, C. J.; Larrea, C. R.; Drevniok, B.; Thanabalasingam, B. Simple direct formation of self-assembled N-heterocyclic carbene monolayers on gold and their application in biosensing. *Nat. Commun.* **2016**, *7*, 12654.
(23) Engel, S.; Fritz, E.-C.; Ravoo, B. J. New trends in the functionalization of metallic gold: from organosulfur ligands to N-heterocyclic carbenes. *Chem. Soc. Rev.* **2017**, *46*, 2057−2075.
(24) Pyykkö, P.; Runeberg, N. Comparative Theoretical Study of N-Heterocyclic Carbenes and Other Ligands Bound to AuI. *Chem.—Asian J.* **2006**, *1*, 623−628.
(25) Hopkinson, M. N.; Richter, C.; Schedler, M.; Glorius, F. An overview of N-heterocyclic carbenes. *Nature* **2014**, *510*, 485−496.
(26) Huynh, H. V. *The Organometallic Chemistry of N-Heterocyclic Carbenes*; John Wiley & Sons, 2017.
(27) Green, M. L. H.; Parkin, G. Application of the Covalent Bond Classification Method for the Teaching of Inorganic Chemistry. *J. Chem. Educ.* **2014**, *91*, 807−816.
(28) Jacobsen, H.; Correa, A.; Poater, A.; Costabile, C.; Cavallo, L. Understanding the M(NHC) (NHC=N-heterocyclic carbene) bond. *Coord. Chem. Rev.* **2009**, *253*, 687−703.
(29) Hurst, E. C.; Wilson, K.; Fairlamb, I. J. S.; Chechik, V. N-Heterocyclic carbene coated metal nanoparticles. *New J. Chem.* **2009**, *33*, 1837−1840.
(30) Ling, X.; Schaeffer, N.; Roland, S.; Pileni, M.-P. Nanocrystals: why do silver and gold N-heterocyclic carbene precursors behave differently? *Langmuir* **2013**, *29*, 12647−12656.
(31) Serpell, C. J.; Cookson, J.; Thompson, A. L.; Brown, C. M.; Beer, P. D. Haloaurate and halopalladate imidazolium salts: structures, properties, and use as precursors for catalytic metal nanoparticles. *Dalton Trans.* **2013**, *42*, 1385−1393.
(32) Vignolle, J.; Tilley, T. D. N-Heterocyclic carbene-stabilized gold nanoparticles and their assembly into 3D superlattices. *Chem. Commun.* **2009**, 7230−7232.
(33) Lara, P.; Rivada-Wheelaghan, O.; Conejero, S.; Poteau, R.; Philippot, K.; Chaudret, B. Ruthenium Nanoparticles Stabilized by N-Heterocyclic Carbenes: Ligand Location and Influence on Reactivity. *Angew. Chem., Int. Ed.* **2011**, *50*, 12080−12084.
(34) Rakers, L.; Martínez-Prieto, L. M.; López-Vinasco, A. M.; Philippot, K.; van Leeuwen, P. W. N. M.; Chaudret, B.; Glorius, F. Ruthenium nanoparticles ligated by cholesterol-derived NHCs and their application in the hydrogenation of arenes. *Chem. Commun.* **2018**, *54*, 7070−7073.
(35) Ranganath, K. V. S.; Kloesges, J.; Schäfer, A. H.; Glorius, F. Asymmetric nanocatalysis: N-heterocyclic carbenes as chiral modifiers of Fe_3O_4/Pd nanoparticles. *Angew. Chem., Int. Ed.* **2010**, *49*, 7786−7789.
(36) Richter, C.; Schaepe, K.; Glorius, F.; Ravoo, B. J. Tailor-made N-heterocyclic carbenes for nanoparticle stabilization. *Chem. Commun.* **2014**, *50*, 3204−3207.
(37) Frogneux, X.; Hippolyte, L.; Mercier, D.; Portehault, D.; Chanéac, C.; Sanchez, C.; Marcus, P.; Ribot, F.; Fensterbank, L.; Carenco, S. Direct Synthesis of N-Heterocyclic Carbene-Stabilized Copper Nanoparticles from a N-Heterocyclic Carbene-Borane. *Chem.—Eur. J.* **2019**, *25*, 11481−11485.
(38) Scholten, J. D.; Ebeling, G.; Dupont, J. On the involvement of NHC carbenes in catalytic reactions by iridium complexes, nanoparticle and bulk metal dispersed in imidazolium ionic liquids. *Dalton Trans.* **2007**, 5554−5560.

https://dx.doi.org/10.1021/acs.chemmater.0c03918
Chem. Mater. 2021, 33, 921−933

(39) Möller, N.; Rühling, A.; Lamping, S.; Hellwig, T.; Fallnich, C.; Ravoo, B. J.; Glorius, F. Stabilization of High Oxidation State Upconversion Nanoparticles by N-Heterocyclic Carbenes. *Angew. Chem., Int. Ed.* **2017**, *56*, 4356−4360.
(40) Rühling, A.; Schaepe, K.; Rakers, L.; Vonhören, B.; Tegeder, P.; Ravoo, B. J.; Glorius, F. Modular Bidentate Hybrid NHC-Thioether Ligands for the Stabilization of Palladium Nanoparticles in Various Solvents. *Angew. Chem., Int. Ed.* **2016**, *55*, 5856−5860.
(41) Díez-González, S.; Marion, N.; Nolan, S. P. N-heterocyclic carbenes in late transition metal catalysis. *Chem. Rev.* **2009**, *109*, 3612−3676.
(42) Hahn, F. E.; Jahnke, M. C. Heterocyclic carbenes: synthesis and coordination chemistry. *Angew. Chem., Int. Ed.* **2008**, *47*, 3122−3172.
(43) Liu, W.; Gust, R. Metal N-heterocyclic carbene complexes as potential antitumor metallodrugs. *Chem. Soc. Rev.* **2013**, *42*, 755−773.
(44) Oehninger, L.; Rubbiani, R.; Ott, I. N-Heterocyclic carbene metal complexes in medicinal chemistry. *Dalton Trans.* **2013**, *42*, 3269−3284.
(45) Martínez-Prieto, L. M.; Ferry, A.; Rakers, L.; Richter, C.; Lecante, P.; Philippot, K.; Chaudret, B.; Glorius, F. Long-chain NHC-stabilized RuNPs as versatile catalysts for one-pot oxidation/hydrogenation reactions. *Chem. Commun.* **2016**, *52*, 4768−4771.
(46) MacLeod, M. J.; Johnson, J. A. PEGylated N-Heterocyclic Carbene Anchors Designed To Stabilize Gold Nanoparticles in Biologically Relevant Media. *J. Am. Chem. Soc.* **2015**, *137*, 7974−7977.
(47) Man, R. W. Y.; Li, C.-H.; MacLean, M. W. A.; Zenkina, O. V.; Zamora, M. T.; Saunders, L. N.; Rousina-Webb, A.; Nambo, M.; Crudden, C. M. Ultrastable gold nanoparticles modified by bidentate N-heterocyclic carbene ligands. *J. Am. Chem. Soc.* **2018**, *140*, 1576−1579.
(48) Narouz, M. R.; Osten, K. M.; Unsworth, P. J.; Man, R. W. Y.; Salorinne, K.; Takano, S.; Tomihara, R.; Kaappa, S.; Malola, S.; Dinh, C.-T.; Padmos, J. D.; Ayoo, K.; Garrett, P. J.; Nambo, M.; Horton, J. H.; Sargent, E. H.; Häkkinen, H.; Tsukuda, T.; Crudden, C. M. N-heterocyclic carbene-functionalized magic-number gold nanoclusters. *Nat. Chem.* **2019**, *11*, 419−425.
(49) Ferry, A.; Schaepe, K.; Tegeder, P.; Richter, C.; Chepiga, K. M.; Ravoo, B. J.; Glorius, F. Negatively Charged N-Heterocyclic Carbene-Stabilized Pd and Au Nanoparticles and Efficient Catalysis in Water. *ACS Catal.* **2015**, *5*, 5414−5420.
(50) Wang, W.; Ji, X.; Du, L.; Mattoussi, H. Enhanced Colloidal Stability of Various Gold Nanostructures Using a Multicoordinating Polymer Coating. *J. Phys. Chem. C* **2017**, *121*, 22901−22913.
(51) Wang, W.; Kapur, A.; Ji, X.; Zeng, B.; Mishra, D.; Mattoussi, H. Multifunctional and High Affinity Polymer Ligand that Provides Bio-Orthogonal Coating of Quantum Dots. *Bioconjugate Chem.* **2016**, *27*, 2024−2036.
(52) Wang, W.; Kapur, A.; Ji, X.; Safi, M.; Palui, G.; Palomo, V.; Dawson, P. E.; Mattoussi, H. Photoligation of an Amphiphilic Polymer with Mixed Coordination Provides Compact and Reactive Quantum Dots. *J. Am. Chem. Soc.* **2015**, *137*, 5438−5451.
(53) Wang, W.; van Niekerk, E. A.; Zhang, Y.; Du, L.; Ji, X.; Wang, S.; Baker, J. D.; Groeniger, K.; Raymo, F. M.; Mattoussi, H. Compact, "Clickable" Quantum Dots Photoligated with Multifunctional Zwitterionic Polymers for Immunofluorescence and In Vivo Imaging. *Bioconjugate Chem.* **2020**, *31*, 1497−1509.
(54) Jin, Z.; Du, L.; Zhang, C.; Sugiyama, Y.; Wang, W.; Palui, G.; Wang, S.; Mattoussi, H. Modification of Poly(maleic anhydride)-Based Polymers with H2N-R Nucleophiles: Addition or Substitution Reaction? *Bioconjugate Chem.* **2019**, *30*, 871−880.
(55) Wang, W.; Ji, X.; Na, H. B.; Safi, M.; Smith, A.; Palui, G.; Perez, J. M.; Mattoussi, H. Design of a Multi-Dopamine-Modified Polymer Ligand Optimally Suited for Interfacing Magnetic Nanoparticles with Biological Systems. *Langmuir* **2014**, *30*, 6197−6208.
(56) Arduengo, A. J., III; Harlow, R. L.; Kline, M. A stable crystalline carbene. *J. Am. Chem. Soc.* **1991**, *113*, 361−363.
(57) Earle, J. M.; Seddon, R. K. Imidazole carbenes. WO 2001077081 A1, 2005.
(58) Susumu, K.; Uyeda, H. T.; Medintz, I. L.; Pons, T.; Delehanty, J. B.; Mattoussi, H. Enhancing the stability and biological functionalities of quantum dots via compact multifunctional ligands. *J. Am. Chem. Soc.* **2007**, *129*, 13987−13996.
(59) Mei, B. C.; Susumu, K.; Medintz, I. L.; Delehanty, J. B.; Mountziaris, T. J.; Mattoussi, H. Modular poly(ethylene glycol) ligands for biocompatible semiconductor and gold nanocrystals with extended pH and ionic stability. *J. Mater. Chem.* **2008**, *18*, 4949−4958.
(60) Wang, W.; Ji, X.; Kapur, A.; Zhang, C.; Mattoussi, H. A Multifunctional Polymer Combining the Imidazole and Zwitterion Motifs as a Biocompatible Compact Coating for Quantum Dots. *J. Am. Chem. Soc.* **2015**, *137*, 14158−14172.
(61) Hiramatsu, H.; Osterloh, F. E. A Simple Large-Scale Synthesis of Nearly Monodisperse Gold and Silver Nanoparticles with Adjustable Sizes and with Exchangeable Surfactants. *Chem. Mater.* **2004**, *16*, 2509−2511.
(62) Liu, S.; Chen, G.; Prasad, P. N.; Swihart, M. T. Synthesis of Monodisperse Au, Ag, and Au-Ag Alloy Nanoparticles with Tunable Size and Surface Plasmon Resonance Frequency. *Chem. Mater.* **2011**, *23*, 4098−4101.
(63) Aslan, K.; Pérez-Luna, V. H. Surface Modification of Colloidal Gold by Chemisorption of Alkanethiols in the Presence of a Nonionic Surfactant. *Langmuir* **2002**, *18*, 6059−6065.
(64) Wang, S.; Du, L.; Jin, Z.; Xin, Y.; Mattoussi, H. Enhanced Stabilization and Easy Phase Transfer of CsPbBr3 Perovskite Quantum Dots Promoted by High-Affinity Polyzwitterionic Ligands. *J. Am. Chem. Soc.* **2020**, *142*, 12669−12680.
(65) Zhang, C.; Palui, G.; Zeng, B.; Zhan, N.; Chen, B.; Mattoussi, H. Non-Invasive Characterization of the Organic Coating of Biocompatible Quantum Dots Using Nuclear Magnetic Resonance Spectroscopy. *Chem. Mater.* **2018**, *30*, 3454−3466.
(66) Mei, B. C.; Oh, E.; Susumu, K.; Farrell, D.; Mountziaris, T. J.; Mattoussi, H. Effects of Ligand Coordination Number and Surface Curvature on the Stability of Gold Nanoparticles in Aqueous Solutions. *Langmuir* **2009**, *25*, 10604−10611.
(67) Agasti, S. S.; You, C.-C.; Arumugam, P.; Rotello, V. M. Structural control of the monolayer stability of water-soluble gold nanoparticles. *J. Mater. Chem.* **2008**, *18*, 70−73.
(68) Jin, Z.; Sugiyama, Y.; Zhang, C.; Palui, G.; Xin, Y.; Du, L.; Wang, S.; Dridi, N.; Mattoussi, H. Rapid Photoligation of Gold Nanocolloids with Lipoic Acid-Based Ligands. *Chem. Mater.* **2020**, *32*, 7469−7483.
(69) Zhukhovitskiy, A. V.; Mavros, M. G.; Van Voorhis, T.; Johnson, J. A. Addressable Carbene Anchors for Gold Surfaces. *J. Am. Chem. Soc.* **2013**, *135*, 7418−7421.
(70) Palui, G.; Aldeek, F.; Wang, W.; Mattoussi, H. Strategies for interfacing inorganic nanocrystals with biological systems based on polymer-coating. *Chem. Soc. Rev.* **2015**, *44*, 193−227.
(71) Smith, C. A.; Narouz, M. R.; Lummis, P. A.; Singh, I.; Nazemi, A.; Li, C.-H.; Crudden, C. M. N-Heterocyclic Carbenes in Materials Chemistry. *Chem. Rev.* **2019**, *119*, 4986−5056.
(72) MacLeod, M. J.; Goodman, A. J.; Ye, H.-Z.; Nguyen, H. V.-T.; Van Voorhis, T.; Johnson, J. A. Robust gold nanorods stabilized by bidentate N-heterocyclic-carbene-thiolate ligands. *Nat. Chem.* **2019**, *11*, 57−63.
(73) Thanneeru, S.; Ayers, K. M.; Anuganti, M.; Zhang, L.; Kumar, C. V.; Ung, G.; He, J. N-Heterocyclic carbene-ended polymers as surface ligands of plasmonic metal nanoparticles. *J. Mater. Chem. C* **2020**, *8*, 2280−2288.
(74) Pyykkö, P.; Runeberg, N. Comparative Theoretical Study of N-Heterocyclic Carbenes and Other Ligands Bound to AuI. *Chem.—Asian J.* **2006**, *1*, 623−628.
(75) Bakker, A.; Timmer, A.; Kolodzeiski, E.; Freitag, M.; Gao, H. Y.; Mönig, H.; Amirjalayer, S.; Glorius, F.; Fuchs, H. Elucidating the Binding Modes of N-Heterocyclic Carbenes on a Gold Surface. *J. Am. Chem. Soc.* **2018**, *140*, 11889−11892.
(76) Young, A. J.; Sauer, M.; Rubio, G. M. D. M.; Sato, A.; Foelske, A.; Serpell, C. J.; Chin, J. M.; Reithofer, M. R. One-step synthesis and XPS investigations of chiral NHC−Au(0)/Au(I) nanoparticles. *Nanoscale* **2019**, *11*, 8327−8333.

(77) Rodríguez-Castillo, M.; Laurencin, D.; Tielens, F.; van der Lee, A.; Clément, S.; Guari, Y.; Richeter, S. Reactivity of gold nanoparticles towards N-heterocyclic carbenes. *Dalton Trans.* **2014**, *43*, 5978−5982.
(78) Westmoreland, D. E.; López-Arteaga, R.; Weiss, E. A. N-Heterocyclic Carbenes as Reversible Exciton-Delocalizing Ligands for Photoluminescent Quantum Dots. *J. Am. Chem. Soc.* **2020**, *142*, 2690−2696.
(79) Du, L.; Arabzadeh Nosratabad, N.; Jin, J.; Zhang, C.; Wang, S.; Chen, B.; Mattoussi, H. Luminescent Quantum Dots Stabilized by N-Heterocyclic Carbene Polymer Ligands. *J. Am. Chem. Soc.* **2021**. DOI: 10.1021/jacs.0c10592, accepted for publication.

https://dx.doi.org/10.1021/acs.chemmater.0c03918
Chem. Mater. 2021, 33, 921−933